Research Square

Preprints are preliminary reports that have not undergone peer review.
They should not be considered conclusive, used to inform clinical practice,
or referenced by the media as validated information.

Lytic polysaccharide monooxygenase (LPMO) expression in Arabidopsis reduces cell wall recalcitrance and boosts immunity against Pseudomonas syringae.

Rajan Kumar Sah
Regional Centre for Biotechnology
Lavi Rastogi
Regional Centre for Biotechnology
Bhagwat Prasad Dewangan
Regional Centre for Biotechnology
Anant Mohan Sharma
Regional Centre for Biotechnology
Prashant Anupama-Mohan Pawar
prashant.pawar@rcb.res.in

Regional Centre for Biotechnology

Research Article

Keywords: LPMO, Pycnoporous coccineus, Arabidopsis thaliana, Saccharification, Lignin, Pseudomonas syringae, immunity, AA14 family

Posted Date: February 24th, 2026

DOI: https://doi.org/10.21203/rs.3.rs-8657892/v1

License: This work is licensed under a Creative Commons Attribution 4.0 International License.
Read Full License

Additional Declarations: No competing interests reported.

Abstract

Background

Lytic Polysaccharide Monooxygenases (LPMOs) are well known for their ability to boost the efficiency of enzyme mixtures used for breaking down lignocellulosic biomass *in vitro*. Nonetheless, the impact of LPMO expression within plants and its influence on cell wall characteristics remains largely unexplored. Several studies have indicated that introducing cell wall degrading enzymes heterologously in plants can enhance saccharification efficiency. Hence, to understand the effects of LPMO expression *in planta*, we introduced the Auxiliary Activity (AA14) family gene from *Pycnoporus coccineus* (*PcAA14*) into *Arabidopsis thaliana*. This was performed using a native signal peptide and was driven by both a constitutive (*35S*) promoter and a xylem-specific (*Cinnamate-4-hydroxylase*) promoter. We then assessed how *PcAA14* expression influenced plant growth, immune response, cell wall composition, and the efficiency of saccharification.

Result

PcAA14 was found to localise to the plasma membrane. Transgenic Arabidopsis lines expressing *PcAA14* accumulated higher levels of oxidized xylo-oligosaccharides relative to wild-type plants after xylanase digestion which confirmed LPMO can be active in plants. Fourier Transform Infrared and mass spectroscopy analysis further revealed presence of oxidized polysaccharides in *PcAA14* expressing plants. Furthermore, these transgenic plants exhibited increased cellulose content and reduced lignin content compared to wild-type. Cell walls from *PcAA14*-expressing plants were more digested by Cellic CTec2 enzymatic cocktail and GH11 xylanase, indicating improved digestibility of major cell wall polysaccharides. Furthermore, expression of *PcAA14* did not result in any observable morphological or anatomical abnormalities instead, these plants observed with improved immunity against *Pseudomonas syringae.*

Conclusion

Our study provides the first evidence that the heterologous expression of LPMO from *PcAA14* in plants enhances the digestibility of cellulose and xylan, both with and without pretreatment. This approach holds promise for tailoring bioenergy crops to support the sustainable production of biobased products.

Background

Lignocellulosic biomass (LCB) is a renewable source that can be used for making valued added bio-products (Sulis et al., 2025). However, the inherent resistant nature of plant cell walls to degradation significantly increases the cost and environmental impact of LCB utilization. Various strategies were employed to reduce recalcitrance of plant cell wall, and the expression of cell wall degrading enzymes

(CWDE) *in planta* has been demonstrated a promising approach to fine-tune the cell wall structure (Chaudhari et al., 2024; Pawar et al., 2016; Rastogi et al., 2021; Swaminathan et al., 2021). Recently, lytic polysaccharide monooxygenase (LPMO) enzymes have gained widespread recognition due to their ability to enhance biomass deconstruction (Vaaje-Kolstad et al., 2010). However, their activity on cell wall polymers was not explored by expressing them in plants. LPMO are a class of copper-containing enzymes that cleave glycosidic bonds of different polysaccharides such as cellulose, hemicellulose, pectin and chitin. LPMO carries out its activity in the presence of oxidative environment and copper in the catalytic site of LPMO gets reduced by long-range electron transfer (Z. Wang et al., 2021). The reduction of copper in the catalytic domain can be achieved by plethora of molecules including O_2, H_2O_2, lignin and ascorbic acid (Vaaje-Kolstad et al., 2010). On the basis of biological origin and substrate specificity, LPMO have been classified into eight auxiliary activity families - AA9, AA10, AA11, AA13, AA14, AA15, AA16, AA17 and AA18 in CAZy database (Kumar et al., 2024). LPMO enzymes show a unique feature which includes activity at wide range of pH and prefer complex substrates for their activity. Also, addition of LPMO in cellulolytic enzyme cocktail can improve the polysaccharide digestibility (Muller et al., 2015). Therefore, *in planta* expression of these enzymes could be a better strategy to reduce cell wall recalcitrance which is explored in this manuscript.

LPMO, which belongs to AA14 family, can oxidize cellulose (Zerva et al., 2020) and cellulose-associated xylan (Couturier et al., 2018) polysaccharides depending the its origin of species (Couturier et al., 2018). Addition of *Pycnoporus coccineus AA14 (PcAA14)* enhances saccharification efficiency in poplar and pine lignocellulosic biomass. Also, synergistic action of xylanases from *Thermothelomyces thermophila* (*TtXyn30A*) and *PcAA14B* released more xylobiose from kraft birchwood cellulosic fibres (Zerva et al., 2020). Moreover, synergistic action of cellobiohydrolases I and II from *Trichoderma longibrachiatum (TlCBHI, TlCBHII)* and *PcAA14B* increases cellobiose release when complex lignocellulosic biomass and microcrystalline cellulose were used as substrate. Interestingly, it was demonstrated that enhancement in saccharification of cellulosic substrate when *Talaromyces rugulosus (TrAA14*) was co-incubated with endoglucanase (GH5). *TrAA14* also prefers both cellulosic and hemicellulosic substrates as its action releases oxidized xylo- and cello-oligosaccharides when fibrillated Eucalyptus pulp was used as substrate (Chen et al., 2024). However, the exact cell wall polymer substrates of *PcAA14* are still under investigation. A recent study reported *PcAA14* could not release oxidized products after incubation with various polysaccharide substrates (Avicel, xyloglucan, Birchwood cellulosic fibres) co-incubated with *PcAA14B* (Tuveng et al., 2023). Therefore, expressing AA14 in plants provides an opportunity to better define the substrate specificity and enzymatic activity of AA14 which have been unclear so far while also demonstrating its potential to enhance plant cell wall properties.

In the present study, we heterologously expressed *Pycnoporous coccineus* LPMO from the AA14 family (*PcAA14*) in Arabidopsis under the control of constitutive and xylem tissue-specific promoters and studied the effect on plant cell wall properties. Our results clearly indicated that *in planta* expression of *PcAA14* improves polysaccharide digestibility and extractability without compromising the plant growth and immunity. We also observed that plants expressing *PcAA14* exhibited reduced lignin content, which may be attributed to the activity of this LPMO in modifying the cell wall, thereby enhancing

saccharification efficiency. Importantly, plant expressing *PcAA14* do not show any abnormalities in plant growth and morphology as compared to wild type plants.

Methods

The growing of Arabidopsis plants

The Arabidopsis Columbia accession (Col-0) was used as the wild type for all the experiments. The root length was measured by growing the seeds on ½ Murashige Skoog Media (MS) which, were surfaced sterilized with 70% ethanol and subsequently washed with autoclaved Milli-Q water. The seedlings grown on plates were kept vertically in growth chamber at 22° C with 16-h light/8-h dark.

Plant phenotyping was also done on soil with similar growth chamber setting.

Cloning and transformation of AA14.

The genes encoding *PcAA14* Lytic Polysaccharide Monooxygenase, (Accession number AUM86167.1) was selected for this study. The codon optimized *PcAA14* was synthesized by Genescript Corporation (Piscataway, NJ, USA) with native signal peptide with HA tag at C-terminal with attL1/attL2 flanking sites in pUC57 cloning vector. To clone into expression vectors, *PcAA14* was amplified (PCWL-346 and 347) using Takara DNA polymerase (Takara Bio companies) ligated into plant binary vectors pCC0995 (containing 35S constitutive promoter), pCC0996 (containing C4H xylem specific promoter) and pSITE-2CA (35S, with N-terminal e-GFP tag) expression vectors using LR clonase (11791020, Thermo Fisher scientific, USA). The colonies were screened for primer PCWL- 495, PCWL-494 and gene specific PCWL-457 primers. The positive colonies were confirmed by sequencing and transformed into Agrobacterium GV3101 strain for stable and transient expression in *Arabidopsis thaliana* and *Nicotiana benthamiana.*

RNA extraction, cDNA preparation, RT-qPCR analysis

Arabidopsis side stem tissue of 6–7-week-old plants were harvested and crushed in liquid nitrogen and stored at -80°C for further use. Total RNA was extracted using TRIzol reagent (15596018, Invitrogen, Canada). Genomic DNA contamination in samples was removed by RNase1- free DNase1 (Cat# EN0601, Thermo scientific, USA). Further, RNA concentration was measured by spectrophotometer (Nanodrop 2000C) and 1 µg of RNA was used for cDNA synthesis using iScript™ kit (Cat. no.1708891, Bio-Rad, USA). RT-qPCR was performed using master mix from Solis BioDyne (8-46-00001, Solis Biodyne, Estonia). The expression of *PcAA14* was measured using gene specific RT-qPCR primers (PCWL-456 and PCWL-457) and *ACTIN2* (PCWL-127 and PCWL-128) was used as reference gene. List of RT-qPCR were listed in **Table S1.** The relative fold change of gene expression compared to reference gene was calculated by ΔΔCT method. Since PcAA14 is not present in wild type, the expression was normalized to one of the transgenic line.

Enzyme activity assay

To determine catalytic production of H_2O_2, freshly harvested plant stem and leaf tissue were harvested and ground in liquid N_2, and suspended into 50 mM Sodium phosphate buffer (pH – 5.8), incubated at 4°C for 30 min. After incubation, the sample mixture was centrifuged at 12000 x g for 10 min and supernatant was named as soluble protein fraction. The pellet was again treated with 50 mM sodium phosphate (pH 5.8) supplemented with 1M NaCl for 30 min at 4°C. Centrifuged at 12000 x g for 10 min at 4°C, separated liquid phase collected, named as wall bound protein fraction. Further measuring H_2O_2 release was performed by Hydrogen peroxide assay kit – Megaplex red (K-MRH2O2, Megazyme, Ireland). This assay is based on formation of coloured product resorufin, from a substrate called Megaplex™ upon oxidation by Horseradish peroxidase (HRP) in the presence of H_2O_2. Sample reaction mixture of assay buffer, protein and Megaplex master mix of Megaplex red, Horse Radish Peroxidase was incubated at room temperature for 30 min and resorufin product was measured at excitation range between 530–560 nm and emission at 590 nm for 0 to 120 min.

Western blot analysis.

Fresh main inflorescence stems from 35S::AA14-HA and C4H::AA14-HA tag expressing plants and wild type were collected, crushed in liquid nitrogen and resuspended in RIPA lysis buffer. The lysate was kept in 4°C for 30 min on shaker. Later centrifuged at 16,000 g and collected supernatant was subjected to quantify the total protein concentration through BCA kit (23225, Thermo Scientific, USA). 50 µg of protein were run on electrophoresis on 12% SDS-PAGE (Sodium Dodecyl Sulphate -Polyacrylamide Gel Electrophoresis) before being transferred to PVDF (Polyvinylidene Difluoride) membrane using a tank transfer method. Then, membrane blocking was done using 5% (w/v) skimmed milk in 1X TBST (Tris-buffered saline with 0.1% w/v Tween 20 detergent) buffer. To detect *AA14* protein, we used anti-HA (3724, Cell Signaling Technology, 1: 5000) and anti-GAPDH (PAB932Mu01, Cloud-Clone Corp., USA, 1:7000) was used as loading control. Blots were imaged under ImageQuant™ LAS 4000 (GE Healthcare).

Subcellular localisation

Agrobacterium containing *35S::GFP-PcAA14* were grown at 28°C, centrifuged at 6000 rpm and resuspended in infiltration medium containing 10 mM MES buffer (RM1128, HiMedia) containing $MgCl_2$, pH 5.6 till 0.4 OD. Furthermore, suspension culture was induced with 100 µM Acetosyringone (RM9145, HiMedia, India) for 4–5 h, leaves of 3-week-old *N. benthamiana* plants were infiltrated and visualised in 40X oil immersion using confocal laser microscopy post 2 days of infiltration.

Cell wall biochemical analyses

To isolate of alcohol insoluble residue (AIR), the inflorescence main stems were harvested, dried, ground in Qiagen tissue lyser (30 Hz, 2 min). Fine crude powder was incubated with 70% ethanol prepared in 4

mM HEPES buffer at 70°C for 30 min, centrifuged at 10,000 g. Pellet was treated with chloroform: methanol (1:1), washed with acetone and vacuum dried overnight. This dried powder was referred as AIR.

Cellulose content

Cellulose content was measured through Updegraff method (Updegraff, 1969). Briefly, 3 mg of AIR was incubated with Updegraff reagent (Acetic acid: Nitric acid: Water, 8:1:2) at 50°C for 3 h. Later, centrifuge at 5000 g to separate soluble and insoluble fraction. Insoluble fraction abundant in cellulosic polysaccharide was treated with 72% H_2SO_4 and sonicated for 15 min. Hydrolysate was further utilised for glucose content analysis through anthrone method.

Lignin content

The total lignin content was measured by acetyl bromide soluble lignin (ABSL) method as described by (Foster et al., 2010). Briefly, 1 mg of AIR was incubated with 25% acetyl bromide (135968, Sigma-Aldrich, Mongolia), freshly prepared in acetic acid (acetyl bromide (1): glacial acetic acid (3) was incubated at 50°C for 2 h and additional 1 h incubation with intermittent shaking. Then samples were cooled down on ice for 10 minutes. Later 400 µL of 2 M NaOH and 70 µL freshly prepared hydroxylamine hydrochloride (159417, Sigma-Aldrich, USA) were added to the reaction mixture. Samples were diluted in glacial acetic acid and absorbance was measured three times at 280 nm.

Lignin measurement after AA14 digestion

The total protein was extracted from stem tissue of WT and *PcAA14* expressing plants. Prior to reaction, the isolated protein was desalted and buffer exchanged with 20 mM sodium acetate buffer pH5.2 using a PD-10 (Sephadex G-25, GE Healthcare) column. Further, 1 mg of wild type Arabidopsis stem AIR was incubated with desalted protein in equimolar concentration for 3 h, at 37°C. Further, washed with Milli-Q water three times and pellet was air dried at room temperature. Later, lignin content in pellet was quantified by ABSL method as explained above.

Monosugars profiling of cell wall

1 mg of AIR was hydrolysed with 100 µL of 1.3 M HCl for 1 h, later neutralised with 100 µL 1.3 M NaOH. Samples were then centrifuged at 1500 g for 10 min at 4°C to separate soluble fraction from remaining insoluble fraction. Further, soluble fraction was diluted 25 times and filtered through 0.22 µm PVDF filter, all assays were carried out in triplicates. These diluted samples were later subjected to HPAEC -PAD (Dionex ICS 6000, Thermo Fischer Scientific, USA) for monosugars profiling as described by (Widmer, 2011). The system was equipped with CarboPac PA1 analytical column (4mm x 250 mm) and CarboPac PA1 guard column (4mm x 50 mm) kept at 30°C. The eluent tubing was connected to freshly prepared

three buffer system (A: 18 mM NaOH, B: 200 mM NaOH, and C: 100 mM NaOH and 150 mM sodium acetate). The optimized and routine gradient used for this method was as follows: 0–7 min, from 100% A; 7–16 min, from 100% A to 70% A and 30% B; 16–18 min, 70%A, 30%B to 6% A, 82% B, and 12% C; 21-23.5 min, from 6% A, 82% B, and 12% C to 100% C; 23.5–27 min, from 100% C to 100% B; 28-39.5 min, from 100% B to 100% A. The sample loop volume was 10 µL. Chromeleon version 7.2.9 was used for instrument control and analysis of ICS-6000. Standard curves were created for each component including fucose, arabinose, rhamnose, galactose, glucose, mannose and xylose over 3 concentration levels (2.5 ppm, 5 ppm, 10 ppm) with replicates.

Detection of xylo-oligosaccharides (XOS) fragments using Dionex 6000 IC system

10 µL of sample were analysed by HPAEC-PAD using CarboPac PA1 analytical column (4mm x 250 mm) and CarboPac PA1 guard column (4 mm x 50 mm). Before injecting samples, the column was equilibrated for 30 mins with 200 mM NaOH solution. Followed by fresh eluents (A: 0.1 M NaOH and B: 0.1M NaOAc, 0.1M NaOH) were prepared as previously described by (Agger et al., 2014; Ostby et al., 2022) and the optimized gradient was as follows: 0–3 min, from 100% A to 94.5% A, 5.5% B; 3–9 min, from 94.5% A, 5.5% B to 85% A, 15% B; 9–20 min, from 85% A, 15% B TO 100% B; 20–26 min, 100% A. The sample loop volume was flushed with 10 µL. Chromeleon version 7.2.9 was used for instrument control and analysis of ICS-6000.

Xylo-oligosaccharide profiling through mass spectroscopy

3 mg of AIR samples were incubated with endo1,4 beta-xylanase (E-XYLAA, Megazyme, Ireland), digested reaction mixture was purified with PGC column (Porous graphitized column, Hypersep Hypercarb 50 mg) and eluted in 50% acetonitrile (Acetonitrile: water) solution. The eluent was freeze dried for 18–20 h. Further, freeze dried sample was resuspended in 600 µL HPLC grade water. The sample supernatant was mixed with equal volume of DHB matrix (stock: 10 mg/ml of 2,5-dihydroxybenzoic acid prepared in 30% acetonitrile) and applied on 384 well ground metal target plate (Opti-TOF LC/MALDI insert (123 x 81 mm) part no. 1018497) and air dried. The data was acquired over the range of m/z 300 to 1500.

Phloroglucinol staining

For light microscopy study, Arabidopsis inflorescence stems were cut transversely into pieces (0.5 to 1 cm, transversely) and fixed in FAA (4% paraformaldehyde, 5% acetic acid, 50% ethanol) solution followed by dehydration in ethanol. The dehydrated samples were embedded in as LR white acrylic resin (L9774, Sigma-Aldrich, USA) and benzoyl peroxide solution (B5907, Sigma-Aldrich, USA) as described (Pradhan Mitra & Loqué, 2014). 10 µm-thick sections were cut using a manual-microtome (RM2125 RTS, Leica, Germany). Further, stained by phloroglucinol-HCl or Wiesner stain.

Fourier Transform Infrared (FTIR)

FTIR spectroscopy was performed on AIR with Nicolet Summit X (912A1139, Thermo Fisher Scientific, USA) coupled with diamond attenuated total reflectance (ATR) crystal. For each sample, 16 scans were acquired ranging in 2000 to 400 cm^{-1} and the resolution was set at 4 cm^{-1}. Omnic paradigm spectroscopy software was used for instrument control and spectroscopy analysis.

Pre-treatment with 0.4 M sodium hydroxide (NaOH)

100 mg of AIR was incubated with 4M NaOH at 90°C for 2 h. After, cooled down on ice, washed with deionised water twice and subsequently washed with acetone. Further, oven dried at 60°C for saccharification analysis.

Pre-treatment with sodium chlorite ($NaClO_2$)

100 mg of AIR was incubated with $NaClO_2$ (1.3%, pH – 3.5) under acidic conditions for 2 h at 75°C. The mixture was centrifuged at 5000 g and separated liquid phase was discarded. Further, pellet was washed with deionised water and acetone sequentially several times. Pellet was oven dried 60°C for further use.

Saccharification assays

Digestibility assay of non-treated AIR, pre-treated AIR was performed with enzymes cellulase (Cellic CTec2) and GH11 xylanase (13814, SRL, India). For digestibility assay with cellulase, 5 mg of cell wall powder (treated or non-treated) was incubated with cellulase (1 µl/mg) at 50°C for 48 h at 750 g on thermomixer. The mixture was centrifuged at 5000 g, separated soluble fraction was diluted 25 times and glucose was measured as explained above Dionex ICS-6000. Similarly, for digestibility assay with GH11 xylanase (13814, SRL, India), 3 mg of AIR1 was treated with xylanase (1 µl/mg) and incubated at 45°C for 24 h at 750 g on thermomixer. Later samples were centrifuged and separated soluble fraction was utilised for detection of glucose and xylose release through Dionex ICS-6000 as described in monosugars profiling section.

ELISA using cell wall specific antibodies

ELISA was performed on alcohol insoluble residue (AIR) as previously described by (Pattathil et al., 2012) with cell wall glycan-specific antibodies. AIR of Arabidopsis main stem was incubated with 50 mM ammonium oxalate, followed by 50 mM sodium carbonate, 1M KOH, and 4M KOH for 24 h each and the reaction products were recovered using stepwise extraction procedure. Fractions were dialyzed and subjected to total sugar estimation through phenol-sulphuric method. Further, fraction was diluted to final concentration of 500 ng/ml. 50 µl from diluted sample was added in ELISA plate and incubated at 37°C. Later, blocked with 1% skimmed milk prepared in 0.1M PBS and incubated with primary antibodies. Further, ELISA plate wells were washed with 0.1% skimmed milk buffer and incubated with secondary antibodies conjugated with horseradish peroxidase (Rastogi et al., 2025).

Plant disease resistance assay

Bacterial strains *Pseudomonas syringae* pv. tomato DC3000 (*Pst DC3000*) was used as a pathogenic strain on *Arabidopsis*. *P. syringae* were grown at 28°C on Pseudomonas agar medium containing 100

µg/mL rifampicin and incubated for 72 h. A tip-full periphery culture was suspended in sterile 10 mM $MgCl_2$ (HiMedia) solution. The bacterial cell density (OD_{600}) was measured using a spectrophotometer, and the colony forming unit (CFU) was adjusted to 1×10^5 for 40 ml. The bacterial suspension was dispensed into the plate containing 14-day-old seedlings, and the bacterial suspension was removed by decantation after incubating for 2–3 minutes at room temperature. The plates containing inoculated plants were sealed and incubated in a growth chamber. Internal bacterial populations were measured at 0 and 3 dpi (Days post infection) to determine bacterial growth in Arabidopsis leaves. Inoculated whole rosettes from seedlings were collected by cutting the hypocotyls to separate the above-agar parts and were washed five times with sterile distilled water. The total weight of inoculated seedlings was measured and then crushed into the MCT using a micro pestle. The sample concentration was adjusted up to 20 mg/mL, and then diluted to 10^{-4} and 10^{-5}. The 50 µl diluted samples were plated on Pseudomonas agar medium containing 100 µg/mL rifampicin and incubated for 48 h. The bacterial CFUs were counted.

Results

Heterologous expression of PcAA14 is possible without affecting plant growth and development in Arabidopsis

Lytic polysaccharide Monooxygenases (LPMO) belong to auxiliary activities (AA) families that prefer complex polysaccharide substrates for their activity. The AA14 family was first assigned to LPMOs from *Pycnoporous coccineus*, which hydrolyse the cellulose-associated xylan (Couturier et al., 2018). Also, the synergistic action of *PcAA14* along with cell wall degrading enzyme cocktails improved saccharification efficiency in pine and poplar wood. Therefore, we wanted to study the effect of heterologous expression of *PcAA14-A* in plants. First, we studied the subcellular localization of *Pc*AA114 tagged with GFP and co-infiltrated in *Nicotiana benthamiana* leaves with RFP-tagged, plasma membrane-localized protein marker. We observed the fluorescence under confocal microscope that showed the distribution of GFP signal in the plasma membrane (Fig. 1a). Further, propidium iodide was used to stain the cell wall and *PcAA14* signal was also found co-localizing with propidium iodide, suggesting its localization either in the plasma membrane or in the cell wall. Additionally, *N. benthamiana* leaf sections were incubated with 30% glycerol to induce plasmolysis, which separates plasma membrane from the cell wall. After plasmolysis, we found GFP signals in the plasma membrane that confirmed *PcAA14* localization in the plasma membrane. Next, we generated transgenic lines of *Arabidopsis thaliana* expressing *PcAA14* under two different promoters that is cauliflower mosaic virus 35S promoter (*35S::PcAA14)* and the Arabidopsis cinnamate 4-hydroxylase (C4H) promoter (*C4H::PcAA14*). Three independent lines of *35S::PcAA14* and *C4H::PcAA14* were selected, i.e., A, H, K, and F, C, D, respectively (Fig. 1b). Morphological studies revealed that transgenic plants expressing *PcAA14* were indistinguishable from wild-type plants at maturation. However, the root length was increased in transgenic lines as compared to the wild-type **(Figure S1)**. We tested the expression of *PcAA14* at RNA level by RT-qPCR. All the lines showed expression of *PcAA14*; among them, H, K, and D were highly expressed compared to the others (Fig. 1c). To confirm protein level expression of *PcAA14* in these transgenic lines, we performed

immunoblot analysis on total protein isolated from highly expressing lines i.e., *35S::PcAA14 (K)* and *C4H::PcAA14 (D).* The *PcAA14* has an HA-tag with a 48 kDa molecular weight, which was detected using an anti-HA antibody, confirming *PcAA14* expression at the protein level in these plants **(**Fig. 1d**)**. Next, we determined LPMO activity in these transgenic lines using Megaplex activity assay, which quantifies the production of H_2O_2. The crude protein was isolated from the stem tissues of *PcAA14*-expressing transgenic lines and relative fluorescence unit (RFU) was calculated by normalizing with total protein concentration. All the transgenic lines showed higher RFU compared to wild-type plants, suggesting higher LPMO activity in *PcAA14*-expressing transgenic plants **(**Fig. 1e**)**. Overall, this data suggested that it is possible to heterologously express *PcAA14* under the control of constitutive and xylem-specific promoters without affecting the plant growth.

Plants expressing PcAA14 can modify xylan structure and change the profile of xylo-oligosaccharides following xylanase digestion.

Since *PcAA14* can release more xylose from pine cell wall and may also form oxidized oligosaccharides (Couturier et al., 2018). Therefore, we digested alcohol insoluble residues of wild-type and transgenic plants with xylanases and released xylo-oligosaccharides (XOS) were detected using High-Performance Anion-Exchange Chromatography with Pulsed Amperometric Detection (HPAEC-PAD). As anticipated, we did not observe any oxidized xylo-oligosaccharides (XOS) following the digestion of beechwood (which contains non-acetylated xylan) and birchwood (which contains acetylated xylan) samples (**Figure S2a and S2b**). In contrast, a clear distinction was noted in the HPAEC-PAD chromatogram profiles of xylanase-digested AIR from wild-type, *35S::PcAA14 (K)*, and *C4H::PcAA14 (D*) plants **(**Fig. 2**)**. Peaks appearing between 12.5 and 16.5 minutes of elution likely represent oxidized xylo-oligosaccharides (XOS), as reported in the literature (Couturier et al., 2018). Because C1-oxidized xylo-oligomers bind more strongly to the HPAEC column, they elute later than non-oxidized oligosaccharides, which is highlighted in the insets of Fig. 2. Relative quantification revealed a more presence of peaks a, b, c, and d in the transgenic lines compared to the wild-type (Table 1). Notably, these peaks were absent in chromatograms of digested purified xylan samples **(Figure S2a and S2b)**. Taken together, these findings indicate that transgenic lines *35S::PcAA14 (K)* and *C4H::PcAA14 (D)* accumulate more oxidized XOS than wild-type plants. To confirm this, xylanase-digested AIR samples were analyzed by matrix-assisted laser desorption ionization (MALDI) – time of flight (TOF) in positive reflector mode according to (Rastogi et al., 2022). Line K showed less abundance of oxidized xylobiose and more abundance of oxidized xylo-tetraose as compared to wild-type plants **(Figure S2c)**. And non-oxidized triose was less abundant in line K as compared to wild-type. The oxidized XOS were comparable in line D as compared to wild-type, however, shift in non-oxidized xylobiose and xylopentaose were also observed **(Figure S2d)**. FT-IR can be used to detect carbonic linkages which are abundant after oxidation of polysaccharides (Sharma et al., 2023). We found that non-digested AIR of transgenic lines K and D showed higher abundance of carboxylic acid linkage at 1735 cm^{-1} as compared to wild-type in crude powder samples which further confirmed the presence of oxidized polysaccharide in *PcAA14* carrying plants as

compared to wild-type plants **(Figure S2e)**. All these data indicated change in xylan structure and probable introduction of oxidized linkages in polysaccharide of *PcAA14*-expressed plants.

Table 1
Quantification of putative oxidised xylooligosaccharide through HPAEC-PAD

Putative Oxidised Xylan	WT	K	D
a) Pu. Ox. Xyl-1	58.4 ± 2.72	99.7 ± 1.25***	88.80 ± 2.59***
b) Pu. Ox. Xyl-2	17.5 ± 6.13	11.8 ± 0.23***	11.30 ± 0.12***
c) Pu. Ox. Xyl-3	22.3 ± 4.10	35.3 ± 0.92***	25.30 ± 1.38*
d) Pu. Ox. Xyl-4	37.0 ± 0.42	71.20 ± 0.17***	62.40 ± 0.47***
Data represent average ± SD, n = 3 or more replicates Student's *t*-test at ***p ≤ 0.01, **p ≤ 0.05, * p ≤ 0.1			

The expression of PcAA14 decreases lignin content and increases in xylan content

Expressing cell wall-degrading enzymes led to changes in cell wall composition (Chaudhari et al., 2024; Pawar et al., 2016). Since *PcAA14*-carrying plants showed changes in cell wall composition by FT-IR, we wanted to perform a detailed analysis of the composition in transgenic lines. The cellulose content was increased in all lines except line C as compared to wild-type plants **(**Fig. 3a**)**. As AA14 is a member of oxygenase family and it is widely known that lignin and other phenols may act as an electron donor for the activity of LPMO (Frommhagen et al., 2017). Therefore, we analyzed the effect on total lignin content, and it was reduced in most of the transgenic lines as compared to wild-type (Fig. 3b). The difference in lignin content was further confirmed by phloroglucinol staining, which specifically stains lignified cells in plant tissue **(**Fig. 3c**)**. The xylem cells of transgenic lines K and D were stained less compared to wild-type plants. To check whether *PcAA14* can directly delignify the cell wall, we isolated total protein from wild-type (WT) and *C4H::PcAA14 (D)*. Later, AIR of WT was treated with these proteins and measured the lignin content. Interestingly, we found decrease in lignin content of wild-type AIR when incubated with *C4H::PcAA14 (D)* protein. However, lignin content was unchanged in *PcAA14* transgenic lines of AIR after incubation with *C4H::PcAA14 (D)* crude protein. To further investigate change in lignin content, we tested the expression of Phenylpropanoid pathway genes and transcription factors -*PHENYLALANINE AMMONIA-LYASE* (*PAL1, PAL2, PAL3), CINNAMATE 4-HYDROXYLASE (C4H), CINNAMYL ALCOHOL DEHYDROGENASE (CAD1, CAD4, CAD5), CINNAMOYL-CoA REDUCTASE (CCR1), 4-COUMARATE CoA LIGASE (4CL1, 4CL3, 4CL5), FERULATE 5-HYDROXYLASE (F5H)*, *MYB46, MYB58 and MYB63.* Although, we observed differential expressions of the above genes in transgenic lines that did not correlate with changes in lignin content **(Figure S3).** This suggested that *PcAA14* may be involved in delignification after polymerization. Further, we analyzed monosugars composition in AIR of *Pc*AA14 transgenic lines and overall, we found increase in xylose content in *35S::PcAA14* (A, H and K) lines and non-cellulosic glucose content was also increased significantly in line A and H as compared to wild type **(**Table 2a**)**. In *C4H:PcAA14* lines, the xylose levels were like those found in wild-type plants, while the amount of non-

cellulosic glucose exhibited an upward trend. (Table 2b). We also found some changes in other monosugars but those were not uniform in all the transgenic lines. Overall, we found significant changes in cellulose, lignin and xylan upon *PcAA14* expression.

Table 2
Monosugar composition analysis on untreated AIR samples

a)	**Fucose**	**Rhamnose**	**Arabinose**	**Galactose**	**Glucose**	**Mannose**	**Xylose**
WT	1.27 ± 0.12	6.71 ± 0.89	6.84 ± 0.60	5.82 ± 0.38	4.52 ± 0.73	0.84 ± 0.07	50.96 ± 1.18
Line A	1.47 ± 0.17**	7.19 ± 0.26	6.91 ± 0.21	5.62 ± 0.11	5.73 ± 0.26***	0.93 ± 0.03**	56.28 ± 0.95***
Line H	1.35 ± 0.07	7.09 ± 0.38	6.91 ± 0.21	5.81 ± 0.13	5.72 ± 0.13**	0.85 ± 0.05	53.92 ± 0.51***
Line K	1.30 ± 0.08	7.11 ± 0.23	6.63 ± 0.44	5.77 ± 0.35	5.25 ± 0.44	1.00 ± 0.01**	55.69 ± 0.61***
b)	Fucose	Rhamnose	Arabinose	Galactose	Glucose	Mannose	Xylose
WT	1.16 ± 0.09	5.64 ± 0.28	5.53 ± 0.26	6.81 ± 0.21	20.97 ± 0.95	6.12 ± 0.17	53.76 ± 0.69
Line F	0.98 ± 0.02	5.38 ± 0.05	5.00 ± 0.19*	6.29 ± 0.16**	22.49 ± 0.67**	6.19 ± 0.05	53.68 ± 0.80
Line C	0.92 ± 0.05	5.19 ± 0.12	4.75 ± 0.13	6.13 ± 0.12	21.88 ± 0.78	6.29 ± 0.09	54.83 ± 0.77
Line D	0.97 ± 0.03	5.42 ± 0.16	4.90 ± 0.12**	6.50 ± 0.19*	21.28 ± 1.03	6.44 ± 0.19	54.49 ± 0.93

Monosugars profiling of main stem expressing *35S:AA14* and *C4H:AA14* . **a)** *and* **b)** without pre-treatment. Abbreviation are as follows, Fuc-Fucose, Rha-Rhamnose, Ara-Arabinose, Gal-Galactose, Glu-Glucose, Man-Mannose, Xyl-Xylose. Data represent average ± SD, n = 3 or more replicates, Student's *t*-test at ***p ≤ 0.01, **p ≤ 0.05, * p ≤ 0.1

Expressing PcAA14 in plants boosts the breakdown of cellulose and xylan, while also increasing resistance to Pseudomonas syringae infection.

As LPMO supplementation improves cellulose and xylan digestibility *in vitro* and heterologous expression of *PcAA14* also showed changes in cell wall properties of Arabidopsis. Therefore, we analyzed saccharification efficiency in transgenic lines after Cellic CTec2 (mixture of cellulase cocktail) and xylanase digestion. The glucose release was increased after Cellic CTec2 digestion in most of the *35S* and *C4H* expressed lines as compared to wild type (Fig. 4a). The highly expressed line K and D showed 22% and 32% increase in glucose release as compared to wild-type plants. However, after treatment with alkali, only highly expressed *35S::PcAA14 (K*) and *C4H::PcAA14 (D*) showed an increase in glucose release after Cellic CTec2 digestion (Fig. 4b). Moreover, AIR was pre-treated with Sodium chlorite to delignify cell wall followed by saccharification (Y. Wang et al., 2021). The PcAA14 expressing

lines H, K, F and D showed increase in glucose release as compared to WT after sodium chlorite treatment (Fig. 4c). After digestion of AIR with xylanase, line K showed 72% increase in xylose release as compared to wild type, whereas Line H, F, C, and D also showed increased xylose release without treatment (Fig. 4d). AIR was treated with NaOH followed by xylanase digestion, and we found increased xylose release in line K and all lines of *C4H::PcAA14* (Fig. 4e). In fact, highly expressed line D showed 97% increase in xylose release as compared to wild-type plants. Xylose release was also increased in transgenic lines as compared to WT after delignification with $NaClO_2$ (Fig. 4F). The analysis of NaOH and $NaClO_2$ fractions by ion chromatography revealed overall higher extraction of xylose in transgenic lines expressing-*PcAA14* (Table 3). The galactose and arabinose levels were less extracted in NaOH and $NaClO_2$ fractions in transgenic lines as compared to WT. Another observation was downregulation of rhamnose levels in $NaClO_2$ fraction of A, H and K. Our data demonstrated that *in planta PcAA14* expression significantly improved cellulose and xylan digestibility with and without treatment.

Table 3
Monosugar composition analysis on pretreated AIR samples

a)	**Fucose**	**Rhamnose**	**Arabinose**	**Galactose**	**Glucose**	**Mannose**	**Xylose**
WT	1.02 ± 0.03	4.74 ± 0.08	4.73 ± 0.11	6.26 ± 0.07	15.85 ± 0.2	4.20 ± 0.10	63.22 ± 0.35
Line A	0.85 ± 0.09**	4.71 ± 0.03	4.50 ± 0.05**	5.80 ± 0.02**	15.70 ± 0.11	4.27 ± 0.04	64.17 ± 0.20**
Line H	0.91 ± 0.08	4.79 ± 0.08	5.04 ± 0.21	6.29 ± 0.11	14.08 ± 0.49	4.03 ± 0.11	64.86 ± 0.64**
Line K	0.93 ± 0.08	4.81 ± 0.06	3.74 ± 0.13	4.89 ± 0.14	16.55 ± 0.87*	3.98 ± 0.13	65.10 ± 0.85**
b)	Fucose	Rhamnose	Arabinose	Galactose	Glucose	Mannose	Xylose
WT	0.82 ± 0.23	4.23 ± 0.16	4.74 ± 0.09	7.24 ± 0.21	15.21 ± 0.78	3.15 ± 0.06	64.62 ± 0.52
Line F	0.77 ± 0.06	4.19 ± 0.05	4.37 ± 0.21*	6.86 ± 0.01**	16.70 ± 0.33**	2.82 ± 0.09**	64.28 ± 0.35
Line C	0.72 ± 0.04	4.34 ± 0.45	4.58 ± 0.29	7.22 ± 0.09	16.30 ± 0.61	2.91 ± 0.10**	63.93 ± 0.70
Line D	0.81 ± 0.03	4.29 ± 0.23	3.86 ± 0.19**	6.67 ± 0.36*	16.84 ± 1.44	3.36 ± 0.30	64.17 ± 1.42
c)	Fucose	Rhamnose	Arabinose	Galactose	Glucose	Mannose	Xylose
WT	1.50 ± 0.38	7.29 ± 0.43	4.67 ± 0.22	6.66 ± 0.18	17.49 ± 0.95	5.32 ± 0.44	57.07 ± 1.77
Line A	1.24 ± 0.07	6.46 ± 0.24**	4.24 ± 0.33	6.07 ± 0.47	16.49 ± 0.46	4.93 ± 0.14	60.57 ± 0.96**
Line H	1.04 ± 0.03	6.64 ± 0.06*	4.40 ± 0.10	6.19 ± 0.07**	16.16. ± 0.47*	4.79 ± 0.11	60.78 ± 0.66**
Line K	1.12 ± 0.04	6.73 ± 0.02*	3.32 ± 0.08*	4.83 ± 0.11**	18.93 ± 1.50	4.78 ± 0.23	60.29 ± 1.55*
d)	Fucose	Rhamnose	Arabinose	Galactose	Glucose	Mannose	Xylose
WT	1.49 ± 0.35	6.93 ± 0.43	4.23 ± 0.16	5.56 ± .07	18.91 ± 0.66	5.06 ± 0.36	57.81 ± 2.01
Line F	1.06 ± 0.03	6.51 ± 0.07	3.76 ± 0.07**	4.98 ± 0.11***	20.77 ± 1.61	4.36 ± 0.04**	58.56 ± 1.45

Monosugars profiling of pre-treated samples of a) and b) with alkali (0.4M NaOH) pre-treatment. c) and d) with 1.3% Sodium Chlorite ($NaClO_2$) pre-treatment. Abbreviation are as follows, Fuc-Fucose, Rha-Rhamnose, Ara-Arabinose, Gal-Galactose, Glu-Glucose, Man-Mannose, Xyl-Xylose. Data represent average ± SD, n = 3 or more replicates, Students t-test at ***p ≤ 0.01, **p ≤ 0.05, * p ≤ 0.1.

a)	Fucose	Rhamnose	Arabinose	Galactose	Glucose	Mannose	Xylose
Line C	0.99 ± 0.06	6.17 ± 0.13	3.62 ± 0.04	5.07 ± 0.07	17.56 ± 0.83	4.54 ± 0.19*	62.04 ± 1.04**
Line D	0.97 ± 0.15*	6.37 ± 0.30	3.37 ± 0.10**	5.25 ± 0.22*	19.18 ± 0.54	5.44 ± 1.04	59.41 ± 0.34

Monosugars profiling of pre-treated samples of a) and b) with alkali (0.4M NaOH) pre-treatment. c) and d) with 1.3% Sodium Chlorite ($NaClO_2$) pre-treatment. Abbreviation are as follows, Fuc-Fucose, Rha-Rhamnose, Ara-Arabinose, Gal-Galactose, Glu-Glucose, Man-Mannose, Xyl-Xylose. Data represent average ± SD, n = 3 or more replicates, Students t-test at ***p ≤ 0.01, **p ≤ 0.05, * p ≤ 0.1.

Additionally, to investigate the extractability of *PcAA14* expressing transgenic plant's cell wall as compared to wild type, we performed glycome profiling using ELISA based screening method. The AIR of WT, *35S::PcAA14 (K)* and *C4H::PcAA14 (D)* were immunolabelled with LM19, LM20, CCRCM7, LM15, LM10, LM11 and LM28 antibodies specific to glycan-specific epitopes. CCRC-M7 antibody recognizes specifically rhamnogalacturonan-1 (RG-1) and more signals were found especially in ammonium oxalate (AOE) and sodium carbonate extraction buffer (SCE) fraction in both the line K and D respectively. We also tested LM19 and LM20 which recognizes non methyl esterified and methyl esterified homogalacturonan (HG) respectively, however signals were comparable wild type and transgenic lines. LM15 which binds to xyloglucan oligosaccharides epitope mostly extracted in 4M KOH fraction and signals were similar in transgenic lines and wild type. However, signals in remaining fractions were enhanced in *35S::PcAA14 (K)* as compared to wild type. LM10, LM11 and LM28 specific to different epitopes of xylan, not major changes observed against these antibodies except less signals were observed against LM11 in 4M KOH fraction of *C4H::PcAA14 (K)* as compared to wild type.

Changes in cell wall properties might also affect plant immunity (Ferrari et al., 2008; Molina et al., 2021). Therefore, all transgenic lines expressing *PcAA14* were flooded with bacterial culture containing 2.5 X 10^3 CFU/ml of *Pseudomonas syringae pv. tomato DC3000* (Fig. 5a). We found same number of bacterial colonies at day 0, whereas a lower number of colonies were observed at day 3 in both *35S::PcAA14* and *C4H::PcAA14* plants compared to the wild type (Fig. 5b). After counting the colonies, we found significantly lower CFU in *PcAA14* transgenic lines compared to wild-type plants (Fig. 5c). This suggested that LPMO expression improves immunity against *Pseudomonas syringae.*

Discussion

Our work provides approach to study the LPMO activity on complex cell wall substrate by expressing *PcAA14* in Arabidopsis which was not explored before. *In-planta* expression of *PcAA14* significantly improves the accessibility for xylan and cellulose; reduces lignin content without damaging plant and xylem vessel morphology. This approach can be further exploited to optimize the cell wall composition of bioenergy crops.

After expression of *PcAA14* under the influence of *35S* and *C4H* promoter, we did not observe any visible difference between transgenic lines as compared to wild-type plants (Fig. 1b). In fact, the root length of transgenic plants was longer than wild-type plants **(Figure S1)**. This has been often observed in lines with modified cell wall composition (Rastogi et al., 2025). Heterologous expression GH10 and GH11 family in poplar changes growth probably through reprogramming hormonal pathways (Sivan et al., 2025). However, the reason for such change's growth has not been explored which could be investigated by transcriptomic, proteomics and metabolomic approaches. We also found improvement in immunity against *Pseudomonas* pathogen in all *PcAA14*-carrying plants (Fig. 5c). Plants expressing *PcAA14* may change endogenous apoplastic oligosaccharide population which might alter immunity in plants. As the supplementation of AA9 LPMO oxidized cello-oligosaccharides in *Arabidopsis thaliana* leaves induces callose deposition, expression immunity related genes and resistance against *Botrytis cinerea* (Zarattini et al., 2021). Similarly, recently identified Auxiliary activity 17 (AA17C) *Phytophthora infestans* causing potato late blight and delineated the importance of *PiAA17C* in causing infection in potato. Silencing *AA17C* from *P. infestans* making it incompetent to infect potato (Sabbadin et al., 2021). However, the function of the oxidised polysaccharides produced in *PcAA14* plants remains to be explored.

Megaplex activity assay determines overall oxygenase activity, which was observed in wild type as well, however, all lines showed increase in hydrogen peroxide (H_2O_2) production as compared to wild type plants. This suggested higher LPMO activity as *PcAA14* carrying plants which was in line with protein level expression confirmed by western blot analysis. The exact activity of LPMO can be determined by analysing the cell wall, the biochemical experiments revealed the presence more xylo-oligomers in *PcAA14* carrying plants after digestion with xylanases (Fig. 2). This correlated with presence of oxidized xylo-oligomers in the elution profile of beechwood cellulosic fibre incubated with *PcAA14A* and GH11 xylanase (Couturier et al., 2018; Ostby et al., 2022). FT-IR analysis also revealed more accumulation C = O linkages which are generated after oxidation of polysaccharides (Sharma et al., 2023) **(Figure S2e)**. Ion chromatography and FT-IR data could not reveal which were the structure of oxidised XOS, this was partially addressed by MALDI-TOF analysis, more accumulation oxidised triose in Line K as compared to WT **(Figure S2c).** We also observed change in pattern of XOS in transgenic lines as compared to wild type, further suggesting LPMO activity in plants (Fig. 2). However, detailed characterization of oxidised oligosaccharides from different polysaccharide such as cellulose will be necessary to further identify preference of *PcAA14.* Such detailed analysis was recently performed to show activity AA17 on pectin (Sun et al., 2025).

Ascorbic acid and gallic acid are well known reductants of LPMO, which are utilised to boost the LPMO activity (Stepnov et al., 2021). Lignin and lignin derivatives can also act as electron donor for the LPMO action (Li et al., 2019; Muraleedharan et al., 2018; Sun et al., 2023; Westereng et al., 2015). Lignin content was reduced in transgenic lines as compared to wild-type plants which was further confirmed reduced lignin content with anatomical studies, with phloroglucinol staining which specifically stain lignin in xylem vessels (Fig. 3c). Additionally, FTIR spectroscopic analysis revealed significant changes in the region 1600 cm^{-1} and 1740 cm^{-1} reflecting C = C and C = O in aromatic components respectively, are

found to be abundant in overexpression lines **(Figure S2e)**. Interestingly, we did not find correlation between gene expression of lignin biosynthetic related genes and decrease in lignin content of transgenic lines. Therefore, we speculate LPMO-mediated decrease of lignin in apoplast in *PcAA14* expressing plants. This is also supported by the fact that lignin can be used as reductant in multiple studies (Frommhagen et al., 2017). Thus, LPMO activity may be exploited to alter polysaccharide and lignin structure to improve cell wall properties.

It is well established that LPMO addition boosts enzymatic saccharification of lignocellulosic biomass (Tang et al., 2024). However, activity of LPMO on polysaccharide digestibility was not explored. *PcAA14* carrying plants showed increase in glucose and xylose release as compared to wild type plants without treatment **(**Fig. 4**)**. The highly expressed *35S::PcAA14 (K)* exhibited maximum accessibility to xylan as compared to other transgenic lines **(**Fig. 4d**)**. This clearly suggests that LPMO expression has open cell wall structure significantly and may convert 2-fold xylan to 3-fold structure which may help in activity of cellulases and xylanases (Zerva et al., 2020). NaOH and $NaOCl_2$ partially solubilises hemicellulosic and lignin respectively. There are very few reports on enhancing saccharification by modifying the xylan backbone through expression of microbial enzymes. Our data correlated with recent data which concluded that expression microbial xylanase from Glycosyl hydrolase family 10 and 11 in poplar improves cellulose and xylan digestibility (Sivan et al., 2025). The NaOH and $NaOCl_2$ soluble sugars did not show major changes in extractability, however, both cellulose and xylan saccharification was increased in transgenic lines again suggesting the primary effect of LPMO heterologous expression on biomass digestibility **(**Fig. 4**).**

Conclusions

AA14 from *Pycnoporous coccinea* can be expressed transiently and stably *in N. benthamiana* and *Arabidopsis thaliana*, respectively, without any visible growth anomaly. *PcAA14* tagged with N-terminal GFP is localized in plasma membrane. *PcAA14* expression and activity is confirmed by qPCR and Megaplex red assay respectively. *PcAA14* carrying plants showed more release of oxidized XOS after xylanases treatment. The reduction in lignin content was probably because *PcAA14* uses lignin as electron donor. All these changes led to positive effect of lignocellulose biomass digestibility as *PcAA14* expressed plants improvement in saccharification efficiency which is summarized in the model (Fig. 6**)**.

Declarations

Consent for publications

All authors have read and approved the manuscript

Authors contributions

RS performed most of the experiments, compiled and analyzed all the data. LR performed western blot analysis, BD performed immunity related assays, AS performed ELISA analysis. RS and PA-MP wrote the

manuscript with input from all the authors. PA-MP conceptualized, designed and secured the funding for the project. All authors read and agree to publish the manuscript.

Acknowledgment

We would like to thank Regional Centre for Biotechnology (RCB) – Advanced Technology Platform Centre (ATPC) for genomics and mass spectroscopy facility.

Funding

We would like to thank Regional Centre for Biotechnology and Anusandhan National research foundation (ANRF/ARG/2025/007339/LS) for funding.

Conflict of Interest

Authors declare no conflict of interest

Data Availability

All data supporting the findings of this study are available within the paper and its Supplementary Information.

References

1. Agger, J. W., Isaksen, T., Varnai, A., Vidal-Melgosa, S., Willats, W. G., Ludwig, R., Horn, S. J., Eijsink, V. G., & Westereng, B. (2014). Discovery of LPMO activity on hemicelluloses shows the importance of oxidative processes in plant cell wall degradation. *Proc Natl Acad Sci U S A*, *111*(17), 6287-6292. https://doi.org/10.1073/pnas.1323629111
2. Chaudhari, A. A., Sharma, A. M., Rastogi, L., Dewangan, B. P., Sharma, R., Singh, D., Sah, R. K., Das, S., Bhattacharjee, S., Mellerowicz, E. J., & Pawar, P. A. (2024). Modifying lignin composition and xylan O-acetylation induces changes in cell wall composition, extractability, and digestibility. *Biotechnol Biofuels Bioprod*, *17*(1), 73. https://doi.org/10.1186/s13068-024-02513-5
3. Chen, K., Zhao, X., Zhang, P., Long, L., & Ding, S. (2024). A novel AA14 LPMO from Talaromyces rugulosus with bifunctional cellulolytic/hemicellulolytic activity boosted cellulose hydrolysis. *Biotechnol Biofuels Bioprod*, *17*(1), 30. https://doi.org/10.1186/s13068-024-02474-9
4. Couturier, M., Ladeveze, S., Sulzenbacher, G., Ciano, L., Fanuel, M., Moreau, C., Villares, A., Cathala, B., Chaspoul, F., Frandsen, K. E., Labourel, A., Herpoel-Gimbert, I., Grisel, S., Haon, M., Lenfant, N., Rogniaux, H., Ropartz, D., Davies, G. J., Rosso, M. N., . . . Berrin, J. G. (2018). Lytic xylan oxidases from wood-decay fungi unlock biomass degradation. *Nat Chem Biol*, *14*(3), 306-310. https://doi.org/10.1038/nchembio.2558

5. Ferrari, S., Galletti, R., Pontiggia, D., Manfredini, C., Lionetti, V., Bellincampi, D., Cervone, F., & De Lorenzo, G. (2008). Transgenic expression of a fungal endo-polygalacturonase increases plant resistance to pathogens and reduces auxin sensitivity. *Plant Physiol*, *146*(2), 669-681. https://doi.org/10.1104/pp.107.109686
6. Foster, C. E., Martin, T. M., & Pauly, M. (2010). Comprehensive compositional analysis of plant cell walls (Lignocellulosic biomass) part I: lignin. *J Vis Exp*(37). https://doi.org/10.3791/1745
7. Frommhagen, M., Mutte, S. K., & Westphal, A. H. (2017). Boosting LPMO-driven lignocellulose degradation by polyphenol oxidase-activated lignin building blocks. *Biotechnol. Biofuels*, *10*, 1.
8. Kumar, A., Singh, A., Sharma, V. K., Goel, A., & Kumar, A. (2024). The upsurge of lytic polysaccharide monooxygenases in biomass deconstruction: characteristic functions and sustainable applications. *FEBS J*, *291*(23), 5081-5101. https://doi.org/10.1111/febs.17063
9. Li, F., Ma, F., Zhao, H., Zhang, S., Wang, L., Zhang, X., & Yu, H. (2019). A Lytic Polysaccharide Monooxygenase from a White-Rot Fungus Drives the Degradation of Lignin by a Versatile Peroxidase. *Applied and Environmental Microbiology*, *85*(9), e02803-02818. https://doi.org/10.1128/AEM.02803-18
10. Molina, A., Miedes, E., Bacete, L., Rodriguez, T., Melida, H., Denance, N., Sanchez-Vallet, A., Riviere, M. P., Lopez, G., Freydier, A., Barlet, X., Pattathil, S., Hahn, M., & Goffner, D. (2021). Arabidopsis cell wall composition determines disease resistance specificity and fitness. *Proc Natl Acad Sci U S A*, *118*(5). https://doi.org/10.1073/pnas.2010243118
11. Muller, G., Varnai, A., Johansen, K. S., Eijsink, V. G., & Horn, S. J. (2015). Harnessing the potential of LPMO-containing cellulase cocktails poses new demands on processing conditions. *Biotechnol Biofuels*, *8*, 187. https://doi.org/10.1186/s13068-015-0376-y
12. Muraleedharan, M. N., Zouraris, D., & Karantonis, A. (2018). Effect of lignin fractions isolated from different biomass sources on cellulose oxidation by fungal lytic polysaccharide monooxygenases. *Biotechnol. Biofuels*, *11*, 1.
13. Ostby, H., Jameson, J. K., Costa, T., Eijsink, V. G. H., & Arntzen, M. O. (2022). Chromatographic analysis of oxidized cello-oligomers generated by lytic polysaccharide monooxygenases using dual electrolytic eluent generation. *J Chromatogr A*, *1662*, 462691. https://doi.org/10.1016/j.chroma.2021.462691
14. Pattathil, S., Avci, U., Miller, J. S., & Hahn, M. G. (2012). Immunological approaches to plant cell wall and biomass characterization: Glycome Profiling. *Methods Mol Biol*, *908*, 61-72. https://doi.org/10.1007/978-1-61779-956-3_6
15. Pawar, P. M., Derba-Maceluch, M., Chong, S. L., Gomez, L. D., Miedes, E., Banasiak, A., Ratke, C., Gaertner, C., Mouille, G., McQueen-Mason, S. J., Molina, A., Sellstedt, A., Tenkanen, M., & Mellerowicz, E. J. (2016). Expression of fungal acetyl xylan esterase in Arabidopsis thaliana improves saccharification of stem lignocellulose. *Plant Biotechnol J*, *14*(1), 387-397. https://doi.org/10.1111/pbi.12393

16. Pradhan Mitra, P., & Loqué, D. (2014). Histochemical staining of Arabidopsis thaliana secondary cell wall elements. *J Vis Exp*(87). https://doi.org/10.3791/51381
17. Rastogi, L., Chaudhari, A. A., Sharma, R., & Pawar, P. A. (2022). Arabidopsis GELP7 functions as a plasma membrane-localized acetyl xylan esterase, and its overexpression improves saccharification efficiency. *Plant Mol Biol*, *109*(6), 781-797. https://doi.org/10.1007/s11103-022-01275-8
18. Rastogi, L., Hussain, M.-M., Tyagi, S., Kabyashree, K., Kharbanda, N., Srivastva, P., Chaudhary, R., Maiti, T. K., Krishnan, V., Jha, G., Voxeur, A., Shrivastava, T., & Pawar, P. A.-M. (2025). Arabidopsis GELP53 overexpression modulates polysaccharide acetylation and defense through oligosaccharide-mediated signaling. *The Plant Cell*, *37*(11). https://doi.org/10.1093/plcell/koaf184
19. Rastogi, L., Singh, D., Sah, R. K., Chaudhari, A. A., & Pawar, P. A.-M. (2021). Enhancement of Biomass for Deconstruction. In *Biomass for Bioenergy and Biomaterials* (pp. 179-210). CRC Press.
20. Sabbadin, F., Urresti, S., Henrissat, B., Avrova, A. O., Welsh, L. R. J., Lindley, P. J., Csukai, M., Squires, J. N., Walton, P. H., Davies, G. J., Bruce, N. C., Whisson, S. C., & McQueen-Mason, S. J. (2021). Secreted pectin monooxygenases drive plant infection by pathogenic oomycetes. *Science*, *373*(6556), 774-779. https://doi.org/doi:10.1126/science.abj1342
21. Sharma, R., Putera, K., Banaszak Holl, M. M., Garnier, G., & Haritos, V. S. (2023). Laccase and LPMO-Driven Biocatalysis Produces Surface Carboxylic Acids on Lignocellulose and Promotes Nanofiber Production. *ACS Sustainable Chemistry & Engineering*, *11*(34), 12541-12551. https://doi.org/10.1021/acssuschemeng.3c01599
22. Sivan, P., Urbancsok, J., Donev, E. N., Derba-Maceluch, M., Barbut, F. R., Yassin, Z., Gandla, M. L., Mitra, M., Heinonen, S. E., Simura, J., Cermanova, K., Karady, M., Scheepers, G., Jonsson, L. J., Master, E. R., Vilaplana, F., & Mellerowicz, E. J. (2025). Modification of xylan in secondary walls alters cell wall biosynthesis and wood formation programs and improves saccharification. *Plant Biotechnol J*, *23*(1), 174-197. https://doi.org/10.1111/pbi.14487
23. Stepnov, A. A., Forsberg, Z., Sørlie, M., Nguyen, G.-S., Wentzel, A., Røhr, Å. K., & Eijsink, V. G. H. (2021). Unraveling the roles of the reductant and free copper ions in LPMO kinetics. *Biotechnology for Biofuels*, *14*(1), 28. https://doi.org/10.1186/s13068-021-01879-0
24. Sulis, D. B., Lavoine, N., Sederoff, H., Jiang, X., Marques, B. M., Lan, K., Cofre-Vega, C., Barrangou, R., & Wang, J. P. (2025). Advances in lignocellulosic feedstocks for bioenergy and bioproducts. *Nat Commun*, *16*(1), 1244. https://doi.org/10.1038/s41467-025-56472-y
25. Sun, P., Peng, M., Csarman, F., Muller, A., Zhang, N., van Berkel, W. J. H., Ludwig, R., de Vries, R. P., & Kabel, M. A. (2025). Oxidative cleavage of methyl-esterified pectic homogalacturonan by an AA17 lytic polysaccharide monooxygenase from Phytophthora infestans. *Carbohydr Polym*, *368*(Pt 2), 124112. https://doi.org/10.1016/j.carbpol.2025.124112
26. Sun, S., Li, F., Li, M., Zhang, W., Jiang, Z., Zhao, H., Pu, Y., Ragauskas, A. J., Dai, S. Y., Zhang, X., Yu, H., Yuan, J. S., & Xie, S. (2023). Lytic polysaccharide monooxygenase synergized with lignin-degrading enzymes for efficient lignin degradation. *iScience*, *26*(10), 107870. https://doi.org/10.1016/j.isci.2023.107870

27. Swaminathan, S., Reem, N. T., Lionetti, V., & Zabotina, O. A. (2021). Coexpression of Fungal Cell Wall-Modifying Enzymes Reveals Their Additive Impact on Arabidopsis Resistance to the Fungal Pathogen, Botrytis cinerea. *Biology (Basel)*, *10*(10). https://doi.org/10.3390/biology10101070
28. Tang, C., Cavka, A., Bui, M., & Jonsson, L. J. (2024). Comparison of simultaneous saccharification and fermentation with LPMO-supported hybrid hydrolysis and fermentation. *Front Bioeng Biotechnol*, *12*, 1419723. https://doi.org/10.3389/fbioe.2024.1419723
29. Tuveng, T. R., Østby, H., Tamburrini, K. C., Bissaro, B., Hegnar, O. A., Stepnov, A. A., Várnai, A., Berrin, J. G., & Eijsink, V. G. H. (2023). Revisiting the AA14 family of lytic polysaccharide monooxygenases and their catalytic activity. *FEBS Lett*, *597*(16), 2086-2102. https://doi.org/10.1002/1873-3468.14694
30. Updegraff, D. M. (1969). Semimicro determination of cellulose inbiological materials. *Analytical Biochemistry*, *32*(3), 420-424. https://doi.org/https://doi.org/10.1016/S0003-2697(69)80009-6
31. Vaaje-Kolstad, G., Westereng, B., Horn, S. J., Liu, Z., Zhai, H., Sørlie, M., & Eijsink, V. G. (2010). An oxidative enzyme boosting the enzymatic conversion of recalcitrant polysaccharides. *Science*, *330*(6001), 219-222. https://doi.org/10.1126/science.1192231
32. Wang, Y., Yang, Y., Qu, Y., & Zhang, J. (2021). Selective removal of lignin with sodium chlorite to improve the quality and antioxidant activity of xylo-oligosaccharides from lignocellulosic biomass. *Bioresource Technology*, *337*, 125506. https://doi.org/https://doi.org/10.1016/j.biortech.2021.125506
33. Wang, Z., Feng, S., Rovira, C., & Wang, B. (2021). How Oxygen Binding Enhances Long-Range Electron Transfer: Lessons From Reduction of Lytic Polysaccharide Monooxygenases by Cellobiose Dehydrogenase. *Angewandte Chemie International Edition*, *60*(5), 2385-2392. https://doi.org/https://doi.org/10.1002/anie.202011408
34. Westereng, B., Cannella, D., Wittrup Agger, J., Jørgensen, H., Larsen Andersen, M., Eijsink, V. G. H., & Felby, C. (2015). Enzymatic cellulose oxidation is linked to lignin by long-range electron transfer. *Scientific Reports*, *5*(1). https://doi.org/10.1038/srep18561
35. Widmer, W. (2011). Analysis of biomass sugars and galacturonic acid by gradient anion exchange chromatography and pulsed amperometric detection without post-column addition. *Biotechnology Letters*, *33*(2), 365-368. https://doi.org/10.1007/s10529-010-0447-x
36. Zarattini, M., Corso, M., Kadowaki, M. A., Monclaro, A., Magri, S., Milanese, I., Jolivet, S., de Godoy, M. O., Hermans, C., Fagard, M., & Cannella, D. (2021). LPMO-oxidized cellulose oligosaccharides evoke immunity in Arabidopsis conferring resistance towards necrotrophic fungus B. cinerea. *Commun Biol*, *4*(1), 727. https://doi.org/10.1038/s42003-021-02226-7
37. Zerva, A., Pentari, C., Grisel, S., Berrin, J. G., & Topakas, E. (2020). A new synergistic relationship between xylan-active LPMO and xylobiohydrolase to tackle recalcitrant xylan. *Biotechnol Biofuels*, *13*, 142. https://doi.org/10.1186/s13068-020-01777-x

Figures

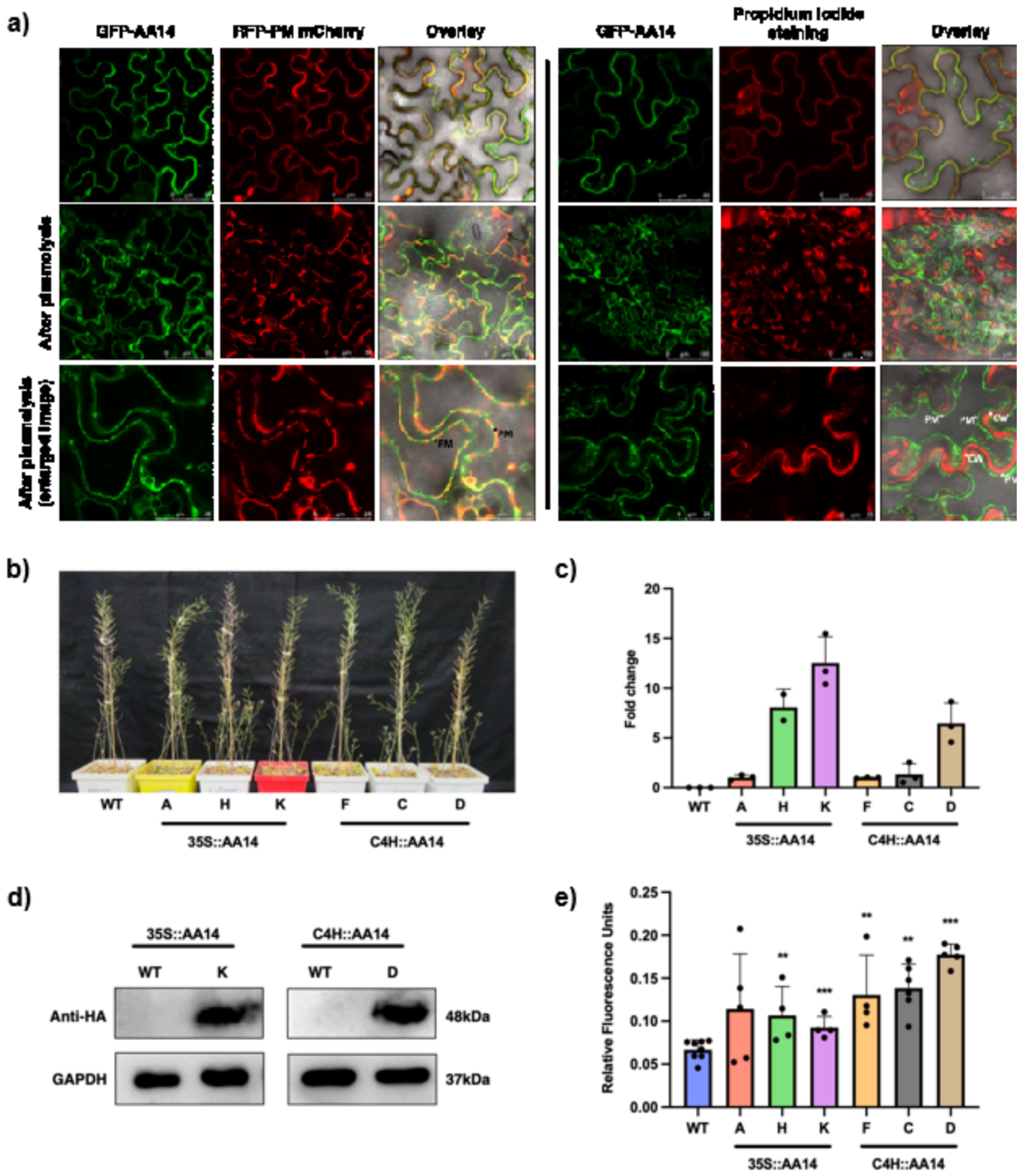


Figure 1

Localization and molecular characterization of *PcAA14* carrying lines

a) Confocal imaging of *PcAA14* in transiently expressing *Nicotiana benthamiana*plants. *PcAA14* was fused with N-terminal GFP (pSITE-2CA) and co-infiltrated with plasma membrane RFP marker in *N. benthamiana* epidermal leaf cells. After 2-days of post infiltration, the leaf sections were visualized under confocal microscope. Leaves were also stained with propidium iodide (PI), and pictures were captured before and after plasmolysis in 30% glycerol with and constitutive (*35S::PcAA14*) and xylem tissue-

specific (*C4H::PcAA14*) promoters, along with the wild type (WT). b) **c)** The gene expression analysis of *PcAA14* from the inflorescence stem of transgenic lines. The expression was normalized to line A with actin as reference gene. **d)**Immunoblot analysis using Anti-HA antibody. GAPDH was used as a loading control. **e)** Comparison of megaplex activity in wild type and *PcAA14*carrying plants. Data represent average ± SD, n = 3, Student's t-test at ***p ≤ 0.01, **p ≤ 0.05, * p ≤ 0.1.

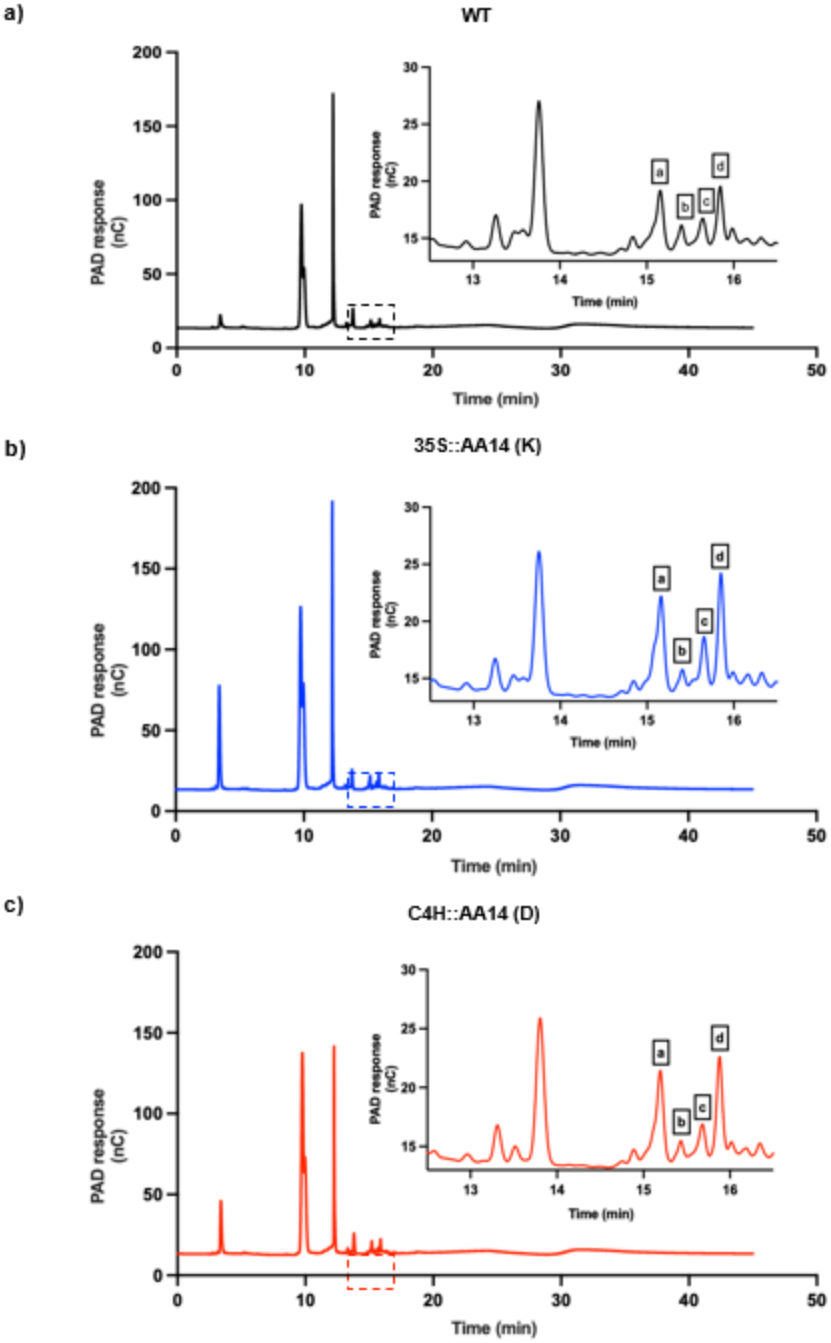


Figure 2

Profiling of xylo-oligosaccharides after xylanase digestion

Alcohol insoluble residue (AIR) was digested with GH11 xylanase from *A. niger* and subjected to ion chromatography. The elution profile of **a)** WT **b)** *35S::PcAA14* (K) **c)** *C4H::PcAA14* are represented. The

inset represents putative oxidised xylo-oligosaccharides, represented by a, b, and c in boxes.

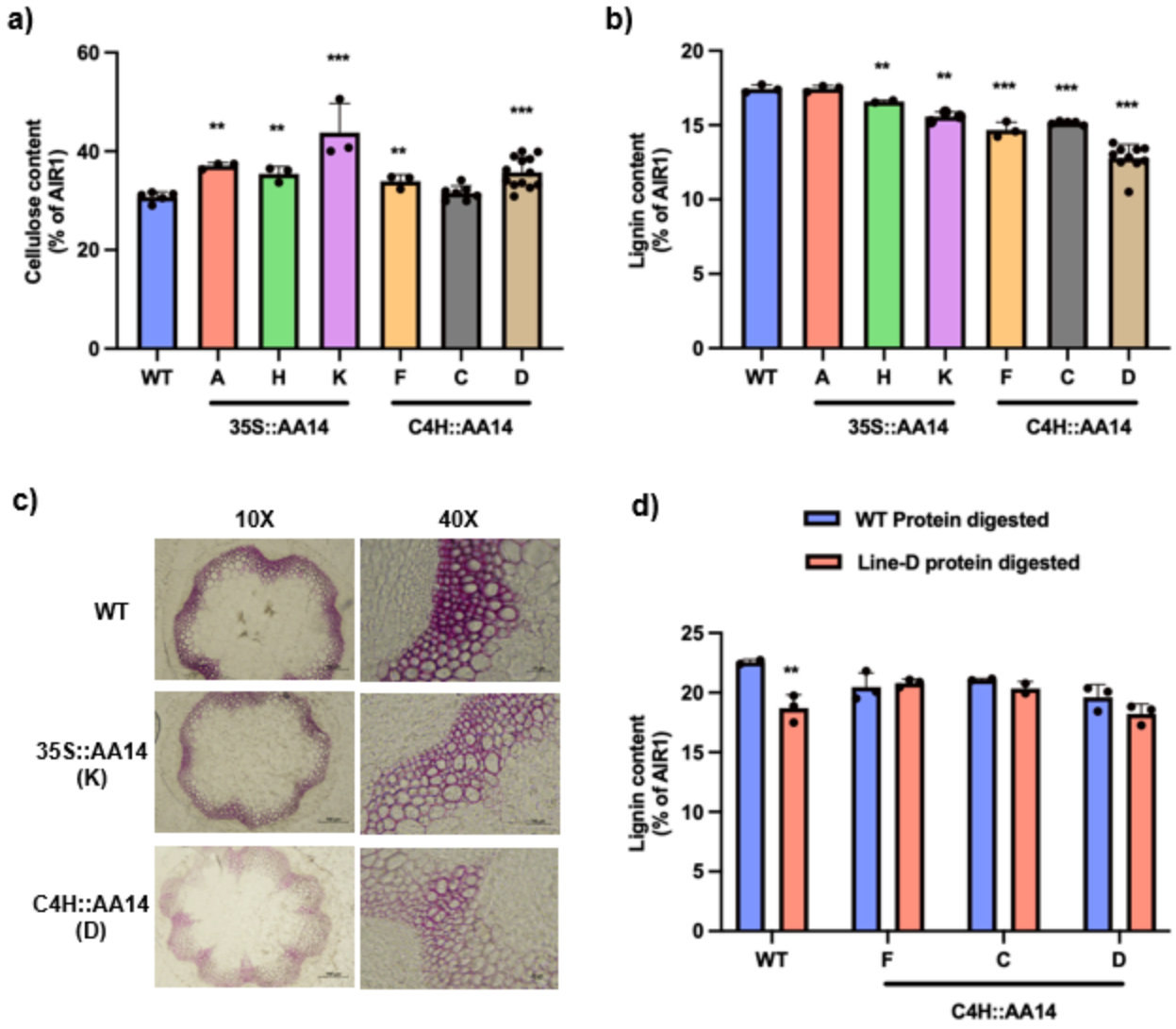


Figure 3

Analysis of cell wall composition on AIR samples prepared from Arabidopsis dried inflorescence stem. **a)** Cellulose content estimation by Updegraff method. **b)** Lignin content estimation by acetyl bromide method (ABSL). **c**) Quantification of lignin (ABSL method) after digesting AIR of WT, with total protein of WT and *PcAA14* expressing lines *C4H::PcAA14* (D). **d)** Transverse section of inflorescence stem of WT, 35S::PcAA14 (K) and *C4H::PcAA14* (D) stained with phloroglucinol stain to visualize lignified cells. Data represent average ± SD, n = 3, Student's *t*-test at ***p ≤ 0.01, **p ≤ 0.05, * p ≤ 0.1.

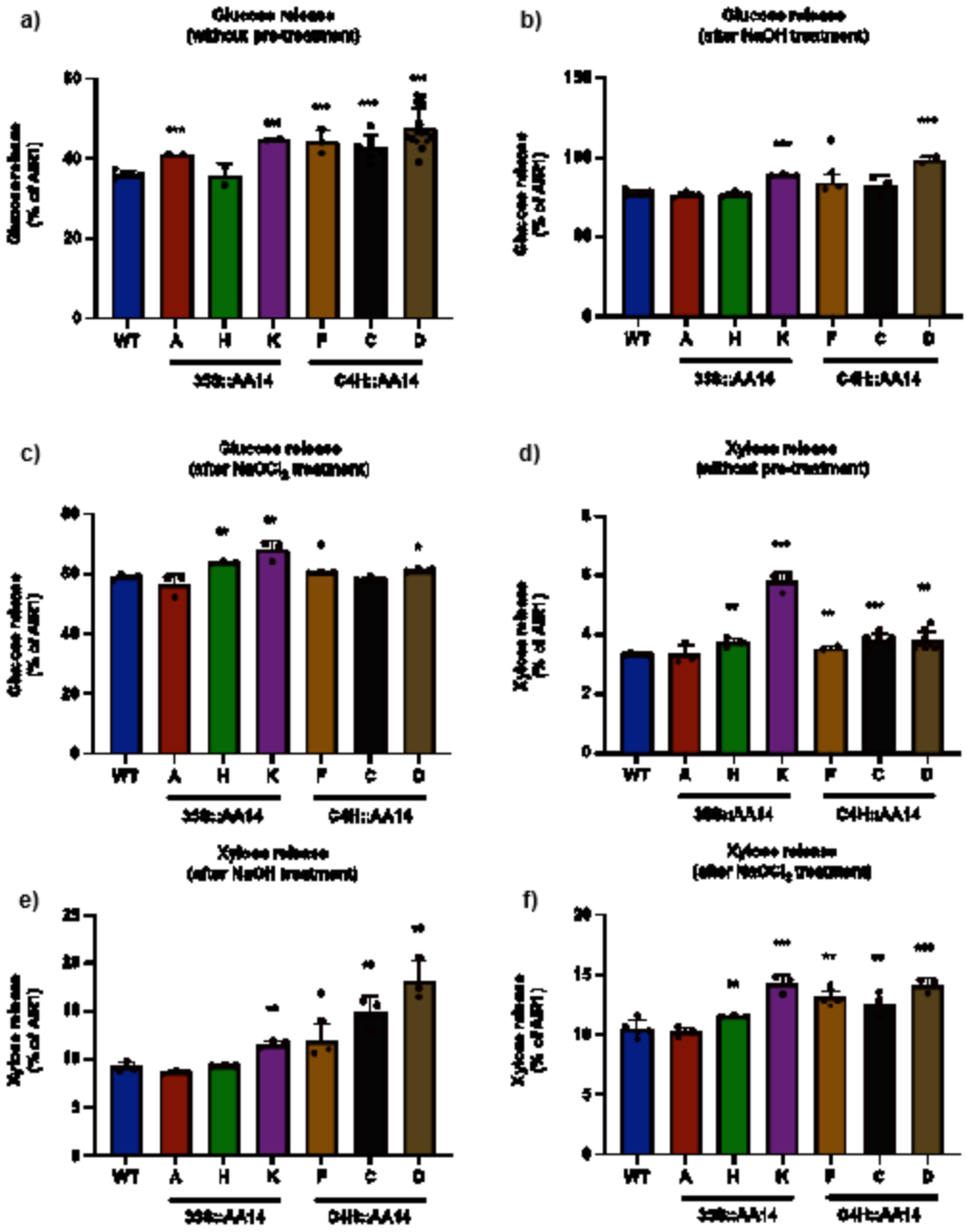


Figure 4

Saccharification analysis of *PcAA14* expressing plants in comparison with wild type. **a)**, **b)** and **c)** digested with Cellic CTec2 enzyme cocktail without treatment **(a)**, with NaOH treatment **(b)** and $NaClO_2$ treatment **(c)**. **d)**, **e)** and **f)** digested with xylanases without treatment **(d)**, with NaOH treatment **(e)** and $NaClO_2$ treatment **(f)**. The release of glucose and xylose after digestion was measured using ion chromatography. The sugar concentration was calculated based on the glucose and xylose standard curve, and the data were represented as % to AIR. Bar diagram represents average ± SD, n = 3 or more replicates, Student's *t*-test at ***p ≤ 0.01, **p ≤ 0.05, * p ≤ 0.1.

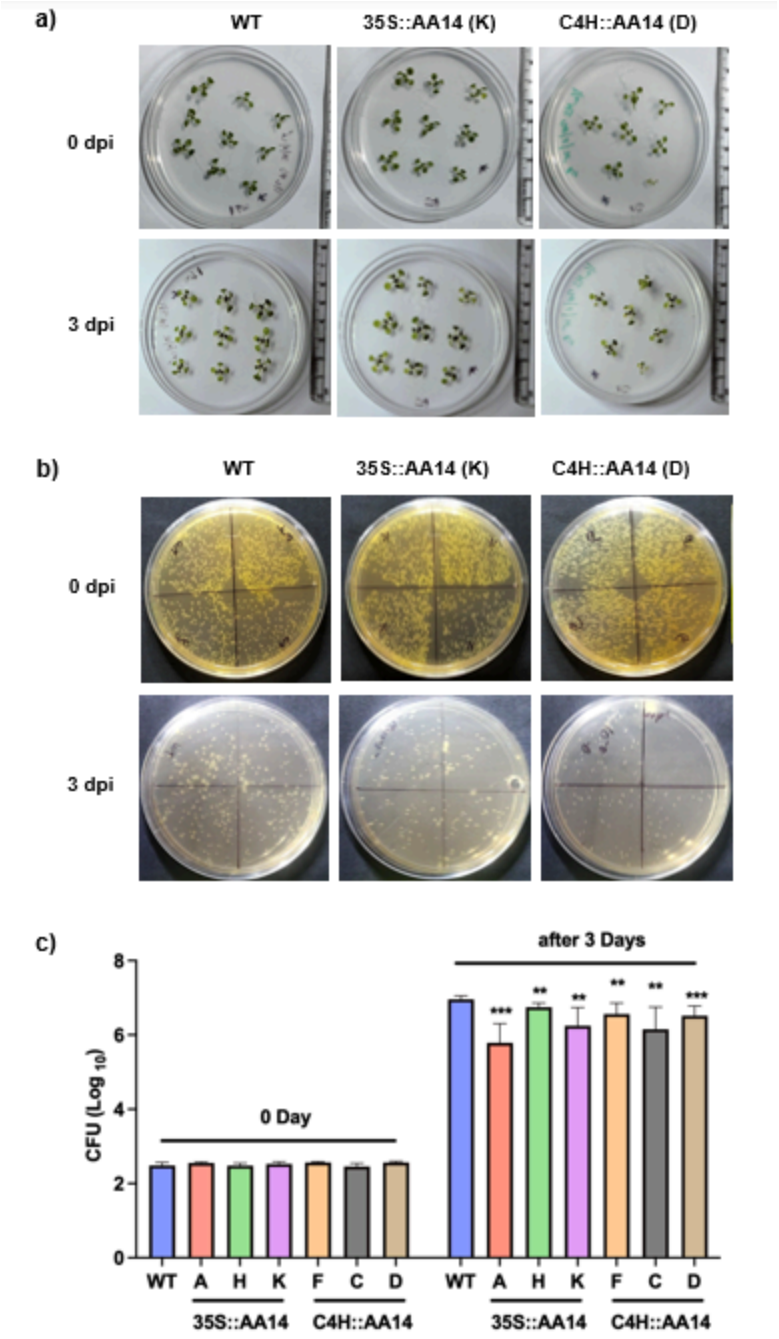


Figure 5

Pathogen assays in seedlings against *P. syringae*

a) Representative of disease phenotype of Arabidopsis seedlings flood-inoculated with bacterial suspension of *P. syringae* at a concentration of 2.5 X 10^3 CFU/ml on 0 day and 3rd day. **b)** and **c)** Bacterial population of *Pst* DC3000 in infected Arabidopsis. Dpi - days post infection, Colony Forming Unit (CFU). Data represent average ± SD, n = 3, Student's *t*-test at ***p ≤ 0.01, **p ≤ 0.05, * p ≤ 0.1.

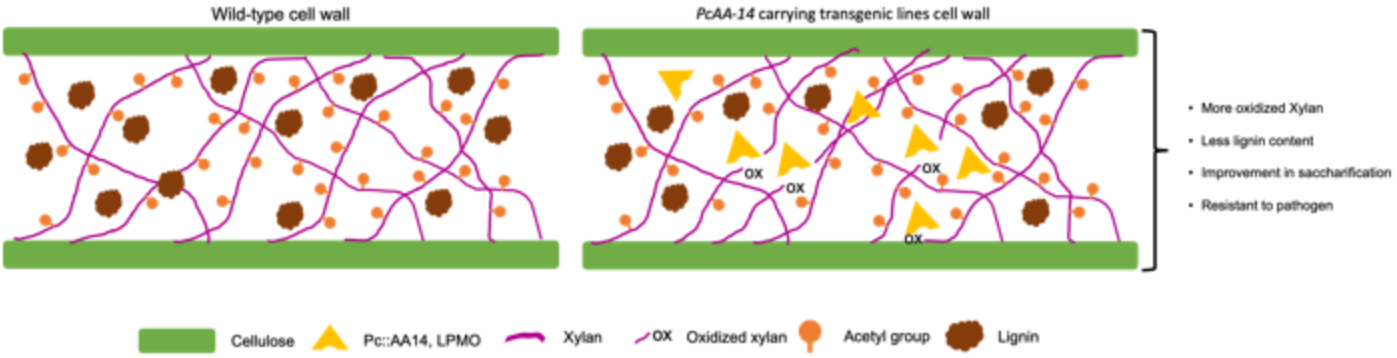


Figure 6

Showing cell wall model of WT and transgenic plants expressing *PcAA14,* under 35S and C4H promoter. *PcAA14*-carrying plants have more oxidized xylo-oligosaccharides (XOS) and less lignin content. These LPMO-driven changes in the cell wall resulted in improved polysaccharide digestibility after cellulase and xylanase treatment in *PcAA14*-carrying plants, compared to the wild type. Additionally, *PcAA14* transgenic lines exhibited resistance to *Pseudomonas syringae*.

Supplementary Files

This is a list of supplementary files associated with this preprint. Click to download.

- SupplementaryfiguresBBBfinal.pptx
- SupplementarytableBBBfinal.docx